European Conference on Computational Fluid Dynamics
ECCOMAS CFD 2006
P. Wesseling, E. Oñate and J. Périaux (Eds)
© TU Delft, The Netherlands, 2006

ENHANCEMENT OF AIRCRAFT CABIN COMFORT STUDIES BY COUPLING OF MODELS FOR HUMAN THERMOREGULATION, INTERNAL RADIATION, AND TURBULENT FLOWS

Johan C. Kok*, Jaap van Muijden*, Sjoerd S. Burgers†, Henry Dol*, and Stefan P. Spekreijse*

*National Aerospace Laboratory NLR,
Anthony Fokkerweg 2, 1059 CM Amsterdam, The Netherlands
e-mail: jkok@nlr.nl, muyden@nlr.nl, dol@nlr.nl,
web page: http://www.nlr.nl/

†Eindhoven University of Technology, Faculty of Mechanical Engineering
P.O. Box 513, 5600 MB Eindhoven, The Netherlands
e-mail: S.S.Burgers@student.tue.nl

Key words: Thermal comfort, Human thermoregulation, Internal radiation, Turbulent flow, Multi-physics coupling

Abstract. *Scientific enhancement of the analysis of thermal comfort aspects in aircraft cabins is the subject of the current investigation. For this purpose, three important processes are identified that play a significant role in thermal comfort, viz. the human response to its thermal environment which is also known as thermoregulation, the actual movement of air and heat inside aircraft cabins due to natural and forced convection, and heat transfer due to radiation. Three existing models have been adopted to describe these phenomena. In the current investigation, the behaviour of these three models is investigated in terms of modelling aspects and computational efficiency. Furthermore, a robust coupling of the models in a single simulation environment is described. Simulation results are shown for academic and real-life applications. It is concluded that a useful simulation environment has been obtained for studying aspects of the individual seat climate. Also, open issues in physical and computational aspects of the models are identified which can be addressed in future studies.*

1 INTRODUCTION

The current air transportation market is still expanding. Passengers all over the world, whether for business or for pleasure, favour the use of airlines as a quick and easy way of getting to their destinations. As air travellers are getting accustomed to the air transportation standards that have prevailed over the past decades, the call for improved transport conditions is becoming louder. As a result, aircraft manufacturers are becoming more and more committed to innovate the air transportation standards during the design phase of new aircraft.

Many aspects play a role in customer satisfaction related to air transportation, e.g., safety, reliability, affordability and comfort. Comfort in itself comprises many aspects, such as seat pitch, noise and vibration levels encountered during flight, the availability of multi-media entertainment, the service level provided by cabin staff, and many more. One important part of customer satisfaction is the perception of thermal comfort, i.e., the individual seat climate which depends on a range of factors. The most important factors involved in thermal comfort are the air temperature, relative humidity, air flow rate, heat radiation and the passenger's activity level and clothing. Investigations regarding individual seat climatisation is part of the European project FACE (Friendly Aircraft Cabin Environment).

In this paper, the development of a computer-based simulation environment to assess aspects of thermal comfort is described. Such an analysis capability can support the design of the cabin interior of modern transport aircraft and their cabin climate control system. In view of the perception of thermal comfort, the simulation environment needs to include physical, physiological and psychological processes. The physical processes are identified as heat exchange mechanisms due to internal cabin flow and heat radiation. The internal cabin flow can arise from natural convection, i.e., due to temperature differences, or from forced convection due to the air conditioning system. Radiative heat exchange occurs due to temperature differences of surfaces inside the cabin such as walls, chairs and clothing of the passenger. The temperature of surfaces can be directly influenced by illumination with sun light through the cabin windows. The physiological process involved is the response and adaptation of the human body to its environment. For the purpose of describing this process, the existing thermoregulation model of Tanabe[13] has been adopted. The psychological process is the actual rating of the passenger of his overall well-being in the thermal cabin environment. Initial studies to arrive at such a rating based on environmental conditions are due to Fanger[4]. In the following, the models for the above sketched processes are described in more detail, and the development of a robust way of coupling these processes is outlined.

2 THERMAL COMFORT

Research related to thermal comfort has been initiated by Fanger[4]. In his work, the thermal state of the human body is determined from a single heat balance equation describing the heat exchange with the environment due to convection and radiation. Measurements of temperatures and heat fluxes have been used to determine realistic coefficients for the convective and radiative heat transfer coefficients. Clothing is described in this approach as a uniform heat resistance. Fanger supplemented this physical heat balance description with experimental investigations, using questionnaires filled in by test persons in climate chambers. In this way, he was able to correlate the thermal state of the human body with actual average ratings of the perception of thermal comfort of a group of people in controlled climate conditions. The thermal comfort indices that arose from his studies are known as 'predicted mean vote' (PMV) and 'predicted percentage of dissatisfied people' (PPD). The PMV-index ranges between -3 and $+3$, with a zero value indicating thermal indifference, a positive value indicating a too warm environment, and a negative value being indicative for a too cold environment. Fanger managed to determine

an expression for the PMV-index as a function of the most important environmental parameters, i.e., the average air temperature, the average air velocity, the mean radiant temperature of the environment, the relative humidity of the air, and the metabolic activity level and clothing of persons in the environment. The PMV-index is an average indicator of the perception of comfort. Due to the fact that people are not alike, there will always be a certain variance in actual thermal sensations around this average. The PPD-index is a direct function of the PMV-index and ranges between 5 percent and 100 percent, reflecting the assumption that at least 5 percent of people in a certain thermal environment will be dissatisfied. Although these comfort indices are widely used and have achieved the status of normative references[7], the basis for the indices are a single heat balance equation and uniform, average environmental conditions. As such, the comfort indices are suitable to represent indoor thermal conditions in buildings, provided the assumption of fairly uniform conditions holds. In the case that non-uniform environments (e.g., due to temperature or air velocity gradients, or due to spatial variation in clothing insulation) need to be correlated with human comfort ratings, the use of these classical indices is no longer trivial.

As noted above, Fanger based his investigations on a single heat balance equation representing a passive description of the heat fluxes to and from the human body. In reality, the human body actively responds to changes in environmental conditions, basically aiming at keeping the body core temperature at a constant temperature of approximately 37 degrees centigrade. The active regulation system is known as the thermoregulation system of the human body. In combination with finite dimensions of the human body and heat balance equations for multiple body segments, an advanced thermoregulation model for the human body can be devised in which it is possible to vary the clothing insulation per body part. Using such a model, a body temperature distribution can be obtained for an average person in a uniform environment. This temperature distribution is not necessarily uniform, and can vary even more due to clothing details. Contrary to Fanger's single-node model, however, such an advanced model also offers possibilities in non-uniform conditions. Further development along these lines of thought leads to the possibility to determine the mutual influence of the human body and the environment by coupling of heat fluxes. In such an integrated approach, the physical heat transfer processes due to fluid flow and radiation need to be modelled in order to obtain a physically correct description of the total heat exchanges.

In the integrated approach it is possible to determine the mutual influence of the human body and the environment. Natural convection will arise due to the heating of air around the human body. Forced convection in a cabin environment can be described using appropriate boundary conditions in inlets and outlets of the air ventilation system. Contrary to Fanger's model, the heat exchange due to convection is not modelled using estimates of averaged heat transfer coefficients but is determined by using the actual flow properties around the body. In similar fashion, the radiative heat transfer is determined using actual surface temperatures. In this way, the multi-physics modelling of the cabin environment leads to the ability to model the spatial and temporal variation of the parameters that are of importance in the assessment of thermal comfort.

3 THERMOREGULATION OF THE HUMAN BODY

As indicated in the previous section, Fanger's heat balance equation models the human body as a single node without true dimensional properties, in which only the steady state of the human body can be represented by averaged properties. Averaged heat fluxes are modelled by heat transfer coefficients based on experimental data. The model does not include any regulation mechanisms of the human body that normally aim at keeping the body temperature at a more or less constant value, even in extreme conditions. A more sophisticated approach is obtained by subdividing the human body into multiple segments. The mutual heat exchange of adjacent body segments and the blood flow then leads to a set of equations describing the thermal state of the human body. The combined heat balance equations of the different body segments form the passive system of the human thermoregulation model. The active part of the thermoregulation model takes care of maintaining an approximately constant body core temperature, around 37 degrees centigrade. Actual active regulation is possible through variations of the heart beat rate and respiration rate, vasodilation and vasoconstriction, and perspiration and shivering.

Several multi-node thermoregulation models consisting of a passive and an active system can be found in literature, e.g., Wissler[16] and Fiala[5,6]. In the current work, the thermoregulation model of Tanabe[13] has been adopted for the purpose of studying aspects of thermal comfort. The Tanabe model contains sixty-five nodes, obtained by modelling four layers of tissue (core, muscle, fat and skin) in sixteen different body segments, supplemented with a central blood compartment as 65th node. The model is based on the earlier Stolwijk model[11,12], which had less segments and an inherently symmetrical description of the thermal state of the human body. The advantage of Tanabe's model is apparent for the modelling of responses to asymmetrical environmental conditions, typical for passengers in a transport vehicle with asymmetrical sunlight loading and asymmetrical air circulation.

The time-dependent heat balance equation, or bioheat equation, for each node takes the general form

$$C\frac{\mathrm{d}T}{\mathrm{d}t} = P - B + E - R - S \tag{1}$$

where C is the heat capacity and T is the temperature of the considered node. On the right hand side, the term P denotes the heat production, B is the heat exchanged with the central blood compartment, E represents the sum of terms denoting the conductive heat exchange with neighbouring nodes, R denotes the heat loss by respiration which is assumed to occur only in the core layer of the chest segment, and S is the total heat loss at the skin surface, which is thus only active at the upper layer of nodes. The heat production consists of the sum of three terms: the basal metabolic rate, the heat production by external work, and the heat production by shivering. Naturally, work and shivering heat production are only available in the muscle layer. The heat transfer of blood flow is depending on the temperature difference between the node and the central blood compartment. It also depends on the blood flow rate, which consists of a basal blood flow rate and a term proportional to the work and shivering performed by the node. The heat loss by respiration is depending on the sum of heat production terms in all nodes. Finally, the total heat loss at the skin surface consists of convective and radiant heat

exchange with the environment as well as evaporative heat loss. The heat exchange with the environment is described by heat-transfer coefficients. The evaporative heat loss is evaluated by two terms, the first one describing the heat loss by water vapour diffusion through the skin, the second one representing the heat loss by evaporation of perspiration. In the first term, the type of clothing plays a role. Values for the heat capacity per node, basal metabolic rates, basal blood flow rate, and other aspects as mentioned above are detailed in Tanabe[13]. In Tanabe[13], also the signals used in the control system part (active part) of the thermoregulation model, responsible for triggering the physiological processes of vasoconstriction, vasodilation, perspiration and shivering, are described. The differences of node temperatures with set-point temperatures, defined as control target temperatures for each node, are an important factor in the determination of signals that trigger the physiological reactions.

It should be noted that Tanabe's model, like many of the similar models, is based on an average man with a weight of $74.43\,\mathrm{kg}$ and a surface area of $1.87\,\mathrm{m}^2$. The heat transfer coefficients describing the exchange of heat with the environment that are used in Tanabe's model when applied in a largely uniform environment have been determined from experiments with thermal manikins.

4 CABIN FLOW

To determine the individual thermal seat climate, an integrated approach is called for in which the thermoregulation model, as discussed in the previous section, is embedded within a computational method to determine the cabin air flow as well as the heat exchange by internal radiation. The use of Computational Fluid Dynamics (CFD) methods is an appropriate choice to model the cabin flow[1,3], but the truly innovative part comes from the integration of all heat sources and heat exchange mechanisms into the simulations. In this section, the NLR in-house developed flow solver ENSOLV[9], which is used to determine the cabin air flow, is briefly described. Radiation is discussed in the next section.

The flow inside an aircraft cabin can be characterized as turbulent, weakly compressible flow containing both forced convection due to the cabin climate control system and natural convection due to buoyancy. This flow is modelled by the compressible Reynolds-averaged Navier–Stokes (RANS) equations, which are closed by the TNT k–ω model[8]. Note that wall-functions are not employed, but the complete boundary layer is resolved instead, requiring mesh sizes at the wall of the order $\Delta y^+ = 1$ (in law–of–the–wall coordinates). The equations are discretized in space by a second-order, cell-centred, finite-volume scheme with fourth-order, matrix-type artificial diffusion for the basic flow equations and a second-order TVD treatment of convective terms in the k–ω equations. To represent complex geometries, multi-block structured grids are employed. The equations are solved by a Full-Approximation Storage (FAS) multigrid scheme that uses Runge–Kutta time integration, accelerated by local time stepping and implicit residual averaging, as relaxation operator.

When applying a compressible flow solver to weakly compressible flow, measures have to be taken to maintain efficiency and accuracy. Efficiency is reduced by the stiffness of the flow equations, caused by a large disparity in wave speeds. This disparity can also result in improper

scaling of the artificial diffusion, reducing the numerical accuracy. To overcome this problem, low-Mach preconditioning is applied to the flow correction of the Runge–Kutta scheme as well as to the artificial diffusion, following Turkel[14,15].

5 INTERNAL RADIATION

The heat exchange through infrared (IR) radiation inside the aircraft cabin is governed by the radiative (heat) transfer equation, which can be found in Siegel & Howell[10]. Depending on the type of thermal radiation, several methods are available for solving this equation. Here, the following modelling assumptions are made:

- All boundaries of the cabin consist of diffuse-grey surfaces of opaque bodies. Opaque means no transmission of radiative energy through the boundaries; diffuse-grey means that emissivity and absorptivity are independent of direction and wavelength.
- The medium inside the cabin (air) does not participate in radiation, i.e., emission and absorption by the medium is negligible. This assumption is valid in case of air at normal humidity levels (water vapour is the main radiatively active air constituent).
- Direct sun light is not taken into account (i.e., the windows are considered to be blinded).
- Heat transfer is instantaneous (compared to the time scales of the flow).

Under these assumptions, the surface-to-surface radiation model is appropriate.

The surface-to-surface model consists of an integral equation, relating the (net) radiation flux leaving the enclosing surface to the temperature distribution of this surface. Let $q_{\text{out}}(\boldsymbol{x})$ be the energy flux per unit area leaving the surface at location $\boldsymbol{x}$, consisting of emitted and reflected energy,

$$q_{\text{out}} = \varepsilon\sigma T^4 + \rho q_{\text{in}}, \tag{2}$$

with $\varepsilon(T)$ the emissivity, σ the Stefan–Boltzmann constant, $T(\boldsymbol{x})$ the surface temperature, $\rho(T)$ the reflectivity, and $q_{\text{in}}(\boldsymbol{x})$ the incident radiation energy flux per unit area. For an opaque body, $\rho = 1 - \alpha$, with α the absorptivity. Furthermore, for a diffuse-grey surface $\alpha = \varepsilon$ (Kirchoff's law). The incident flux is obtained by accumulation of all fluxes arriving at the current location,

$$q_{\text{in}}(\boldsymbol{x}) = \int_{\boldsymbol{y}\in\partial D} K(\boldsymbol{x},\boldsymbol{y}) q_{\text{out}}(\boldsymbol{y}) \mathrm{d}S, \tag{3}$$

with ∂D the enclosing surface and with $K(\boldsymbol{x},\boldsymbol{y})$ a geometric quantity called the kernel. The kernel determines the visibility between two distinct locations of the surface and depends on the local orientation of the surface and on the distance between the two locations. Substitution of equation (3) in equation (2) gives an integral equation for q_{out}. The net radiation flux leaving the surface is simply given by $q_{\text{r}} = q_{\text{out}} - q_{\text{in}}$.

A simplification of the surface-to-surface model is the net-radiation method in which the surface is divided into a limited number of large panels with uniform radiation flux, temperature,

and emissivity. A limited set of equations is then obtained, relating the net fluxes and temperatures of the panels. The equations depend on the so-called configuration factors (or view factors), which determine the visibility between two panels and which are obtained by integrating the kernel over the two panels. Through the years, configuration factors have been tabulated for many elementary geometrical configurations, which can be combined using configuration-factor algebra[10]. The net-radiation method was used by Fanger[4] in his pioneering thermal comfort studies, and, in fact, it is still the recommended (building) engineering approach[2,7].

With present-day computer power, there is no need to simplify the surface-to-surface model. It can be solved directly by standard numerical methods. In the current approach, the integral equation is discretized on the structured surface grid that is obtained from the 3D multi-block grid used to solve the flow equations. This facilitates the direct exchange of fluxes and temperatures between the radiation and the flow model. As for the net-radiation method, configuration factors are needed, but now between grid cell faces along the surface (rather than between comparatively large panels). These configuration factors do not need to be analytically exact, but only need to be consistent in the limit of zero mesh size. Here, they are computed by a contour integral along the emitting cell faces.

After discretization of the surface-to-surface model, a large set of linear equations is obtained. Let the size of the 3D multi-block grid be $\mathcal{O}(N^3)$, with N the number of cells in one direction. The number of surface cell faces is then $\mathcal{O}(N^2)$. As each discrete equation relates a cell face to all other cell faces, the size of the linear system is $\mathcal{O}(N^4)$. Thus, for large values of N, both the storage and the computation of the non-sparse matrix of the system (i.e., the configuration factors) will become the main bottleneck.

For the computation of the configuration factors, an important complication is the possible presence of obstacles between the panels (third-body shadowing). Straightforward computation of shadowing can become extremely expensive. If, for each pair of cell faces, it is checked whether or not every other cell face forms an obstruction, then the number of required operations is $\mathcal{O}(N^6)$. To determine the shadowing, commercial software is available.

To keep the size of the surface-to-surface model within reasonable limits, optionally the discrete radiation equations are applied to a coarser grid level than the flow equations. A coarse grid level is obtained by joining 2×2 (or 4×4, etc.) cell faces into one coarse cell face.

6 COUPLING METHODOLOGY

In this section, the coupling of the flow model with the thermoregulation model and the surface-to-surface radiation model is described. The coupling approach is essentially depicted in figure 1. In this approach, the thermoregulation and radiation models are each coupled with the flow model, but not directly with each other. Therefore, the two models can be considered separately.

The radiation model computes the net radiation flux leaving the surfaces enclosing the flow domain, given the temperatures of these surfaces. This model is coupled with the flow model by passing the net radiation flux (q_r) to the flow model, where it is used in the temperature boundary condition, and by passing the temperature from the flow model to the radiation model

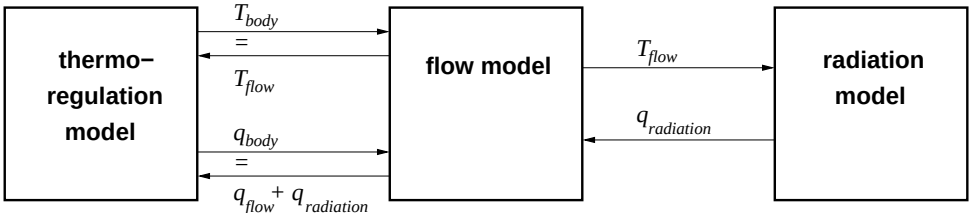

Figure 1: Coupling of the flow model with the thermoregulation model and the surface-to-surface radiation model.

to compute the net radiation flux. Both the non-linear flow equations and the linear radiation equations are solved by iterative schemes. For the flow equations, a (full-approximation storage) multi-grid scheme is used. Each fine-grid relaxation of the multi-grid scheme is preceded by one iteration of the radiation model. As the radiation model consists of a diagonally dominant linear system, it is solved by simple Jacobi iterations.

The thermoregulation model consists of a set of equations for the temperature distribution (in terms of 65 nodes) of the human body. This set of equations can be interpreted as a non-linear model relating the heat flux (q_b) through the body surface, with the temperature (T_b) of the body surface (i.e., the surface of the clothes or the naked skin), formally written as

$$\mathcal{T}(q_b, T_b) = 0. \tag{4}$$

Similarly, the set of flow equations can be interpreted as a non-linear model relating the thermal-diffusion heat flux (q_f) at the surfaces enclosing the flow domain with the temperature (T_f) at these surfaces,

$$\mathcal{F}(q_f, T_f) = 0. \tag{5}$$

The two systems are closed by requiring that the temperature at the body surface is unique and that the body heat flux equals the sum of the thermal-diffusion flux and the radiation flux:

$$T_b = T_f, \tag{6a}$$

$$q_b = q_f + q_r(T_f). \tag{6b}$$

Thus, four equations for four dependent variables are obtained.

To solve the complete set of equations, several approaches are possible. One option is to solve the thermoregulation model with the body heat flux (equation (6b)) as boundary condition and to solve the flow model with the body temperature (equation (6a)) as boundary condition. However, in practice this approach was found to be unstable. A stable approach consists of the so-called quasi-simultaneous method. Both models are solved with as boundary condition a linearization of the other model (also sometimes called an interaction law). This linearization can be written in terms of heat-transfer coefficients. Define the body heat-transfer coefficient (h_b) and the flow heat-transfer coefficient (h_f) as

$$h_b = \frac{q_b}{T_{\text{core}} - T_b}, \tag{7a}$$

$$h_f = \frac{q_f + q_r}{T_f - T_\infty}, \tag{7b}$$

room height	L	$= 2.4\,\mathrm{m}$
gravitational constant	g	$= 9.81\,{}^{\mathrm{m}}/_{\mathrm{s}^2}$
inflow velocity	u_{ref}	$= 0.629\,{}^{\mathrm{m}}/_{\mathrm{s}}$
inflow temperature	T_{ref}	$= 296.15\,\mathrm{K}$ (= $23\,^{\circ}\mathrm{C}$)
inflow density	ρ_{ref}	$= 1.205\,{}^{\mathrm{kg}}/_{\mathrm{m}^3}$
specific heat at constant pressure	c_p	$= 1007\,{}^{\mathrm{J}}/_{(\mathrm{kg\,K})}$
dynamic viscosity	μ_{ref}	$= 1.82 \cdot 10^{-5}\,\mathrm{Pa\,s}$
thermal conductivity	λ_{ref}	$= 0.0257\,{}^{\mathrm{W}}/_{(\mathrm{mK})}$
Stefan–Boltzmann constant	σ	$= 5.6704 \cdot 10^{-8}\,{}^{\mathrm{W}}/_{(\mathrm{m^2K^4})}$
emissivity	ε	$= 0.9$

Table 1: Parameters of flow and radiation for a seated man in a ventilated room.

with T_{core} the temperature at the core of the human body and T_∞ a suitable reference temperature of the flow field. The thermoregulation model is now solved using the boundary condition

$$q_b = h_f(T_b - T_\infty), \tag{8}$$

with a fixed value of h_f obtained from the flow model. Similarly, the flow model is solved using the boundary condition

$$q_f + q_r = h_b(T_{\text{core}} - T_f), \tag{9}$$

with a fixed value of h_b obtained from the thermoregulation model. Alternate iteration steps are taken for the flow and the thermoregulation models, with each multi-grid cycle for the flow equations being preceded by several Runge–Kutta time steps (with local time stepping) for the thermoregulation model. Note that the conditions of equation (6) are only satisfied once the complete set of equations has converged.

7 RESULTS

7.1 Man in ventilated room

To test the full coupling of all three models (flow, radiation, and thermoregulation) a seated man in a ventilated room is considered. Air enters the room at the upper right-hand side (relative to the man) and leaves the room at the bottom left-hand side. The temperature (and heat fluxes) at the body surface are determined by coupling of the flow and radiation models with the thermoregulation model. At the other surfaces (cabin walls and chair surface), adiabatic conditions are prescribed. The relevant parameters that have been used to specify the flow model and the radiation model are given in table 1. Note that a constant emissivity has been assumed along all surfaces. For the thermoregulation model, a metabolic rate of the whole body of $1.2\,\mathrm{met}$ (light activity) and a relative humidity of the air of 30% has been assumed.

A multi-block structured grid has been generated that consists of 152 blocks and 2.84 million grid cells. In order to keep the memory requirements for the configuration factors of the radiation model within acceptable limits, the radiation equations are solved on the surface grid that is one level coarser.

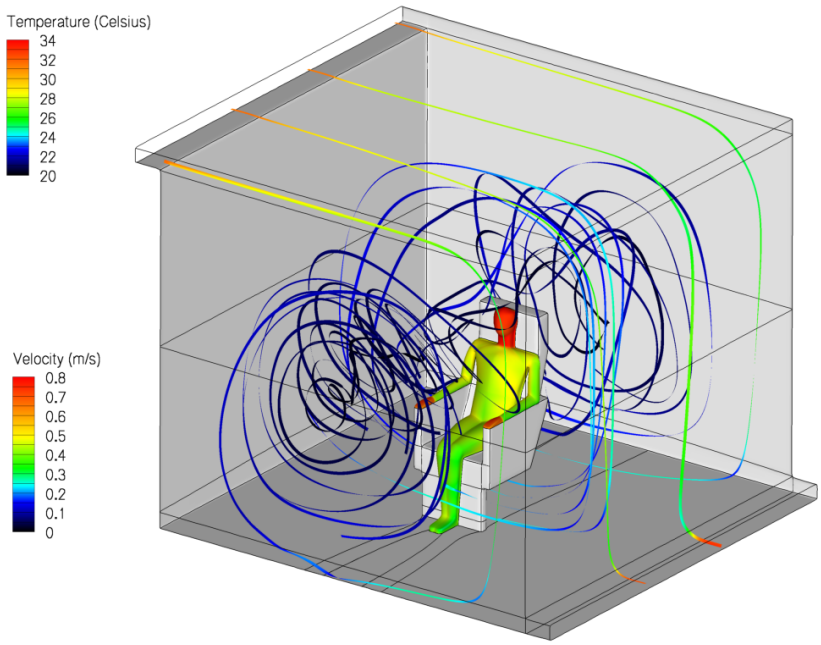

Figure 2: Impression of flow solution for a seated man in a ventilated room. Body surface is coloured with temperature. Stream traces are coloured with local air velocity.

The following procedure has been used to perform the computations. First, a solution to the original thermoregulation model is obtained for a man in a quiescent environment (with ambient temperature $T_{\text{amb}} = 23\,^{\circ}\text{C}$). The original model is not coupled with the flow and radiation models, but fixed flow and radiation heat transfer coefficients are used (obtained from thermal manikin experiments, Tanabe[13]). Then, the flow and radiation models are solved with fixed body-surface temperatures as obtained from the original thermoregulation model and with an inflow temperature $T_{\text{ref}} = T_{\text{amb}}$. Starting from this solution, a coupled simulation is performed for the complete system. Finally, also a coupled simulation is performed with a reduced inflow temperature $T_{\text{ref}} = 18\,^{\circ}\text{C}$.

An impression of the flow solution is given in figure 2. The stream traces show the circulation around the man, caused by the forced convection (from inflow to outflow boundaries) and by buoyancy. In the vicinity of the man, flow velocities appear to be highest near his legs.

The body-surface temperature distributions obtained from the original thermoregulation model and from the coupled simulations are shown in figure 3. Note that the coupled simulations allow non-constant temperature per body segment, contrary to the original thermoregulation model. The body temperatures of the original thermoregulation model and the coupled simulation with $T_{\text{ref}} = T_{\text{amb}}$ are in fair agreement. This implies that, in this situation, the effective heat transfer coefficients resulting from the coupled simulation must be close to the coefficients from the thermal manikin experiments. These latter coefficients only include the effects of natural convection (due to buoyancy) and radiation and not the effect of forced convection. Thus, the effect of forced convection appears to be limited for this case. However, lower temperatures

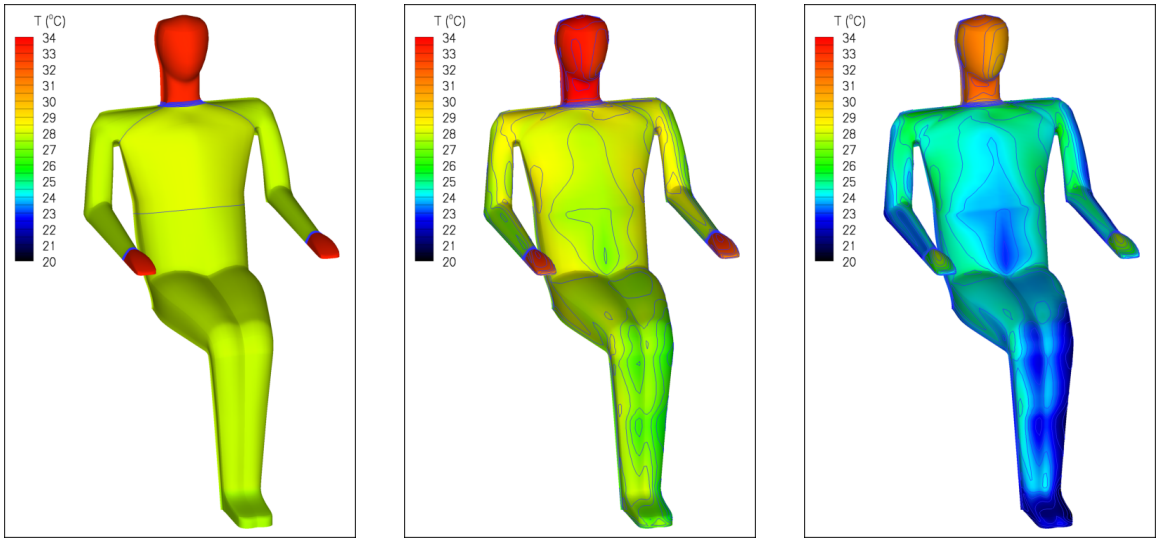

(a) Thermoregulation model with ambient temperature $T_{\text{amb}} = 23\,^{\circ}\text{C}$ (b) Coupled system with inflow temperature $T_{\text{ref}} = 23\,^{\circ}\text{C}$ (c) Coupled system with inflow temperature $T_{\text{ref}} = 18\,^{\circ}\text{C}$

Figure 3: Body-surface temperature distribution of a seated man in a ventilated room.

are observed along the outside arms and the lower legs. Furthermore, the left side appears to be cooled more strongly than the right side, as can also be seen from the heat fluxes given in figures 4 and 5. This is the most evident for the thermal-diffusion heat flux (which is more directly related to the effect of the forced convection than the radiation heat flux). The stronger cooling of the left side can be related to the strong downward draft on the left side of the room.

The convergence of the coupled simulations are shown in figure 6. Note that per iteration of the flow model, ten iterations are performed for the thermoregulation model. The body-surface temperatures of the thermoregulation and flow models have different values during the iterative scheme, but rapidly convergence to each other. The same is true for the heat fluxes (not shown).

7.2 Cabin with passenger

As a final test case, a cabin section is considered that consists of one row of six chairs. Only half the configuration is used (assuming symmetry) with one seated passenger. The air conditioning system blows the air into the cabin such that the complete volume is replaced in approximately two minutes. As for the ventilated room, the temperature (and heat fluxes) at the body surface are determined by coupling of the flow and radiation models with the thermoregulation model. At the cabin walls and chair surfaces, adiabatic conditions are prescribed. A symmetry condition is applied at the central symmetry plane, while periodic conditions are applied at the fore and aft planes. The relevant parameters are given in table 2. Again, for the thermoregulation model, a metabolic rate of the whole body of $1.2\,\text{met}$ (light activity) and a relative humidity of the air of 30% has been assumed.

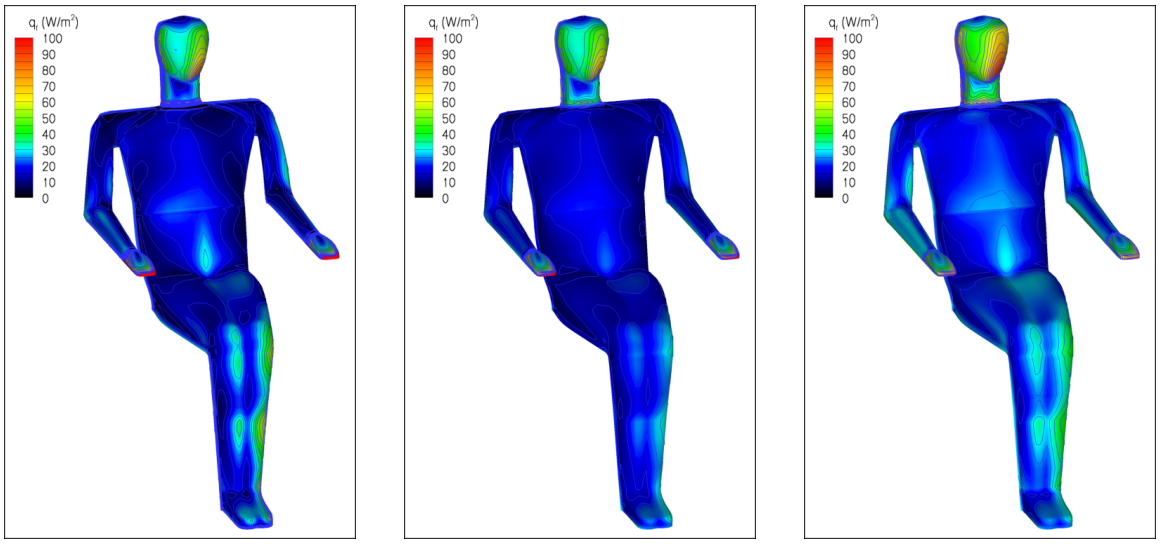

(a) Flow and radiation models with fixed body-surface temperature (of thermoregulation model with ambient temperature $T_{\text{amb}} = 23\ ^\circ\text{C}$)

(b) Coupled system with inflow temperature $T_{\text{ref}} = 23\ ^\circ\text{C}$

(c) Coupled system with inflow temperature $T_{\text{ref}} = 18\ ^\circ\text{C}$

Figure 4: Distribution of thermal-diffusion heat flux for a seated man in a ventilated room.

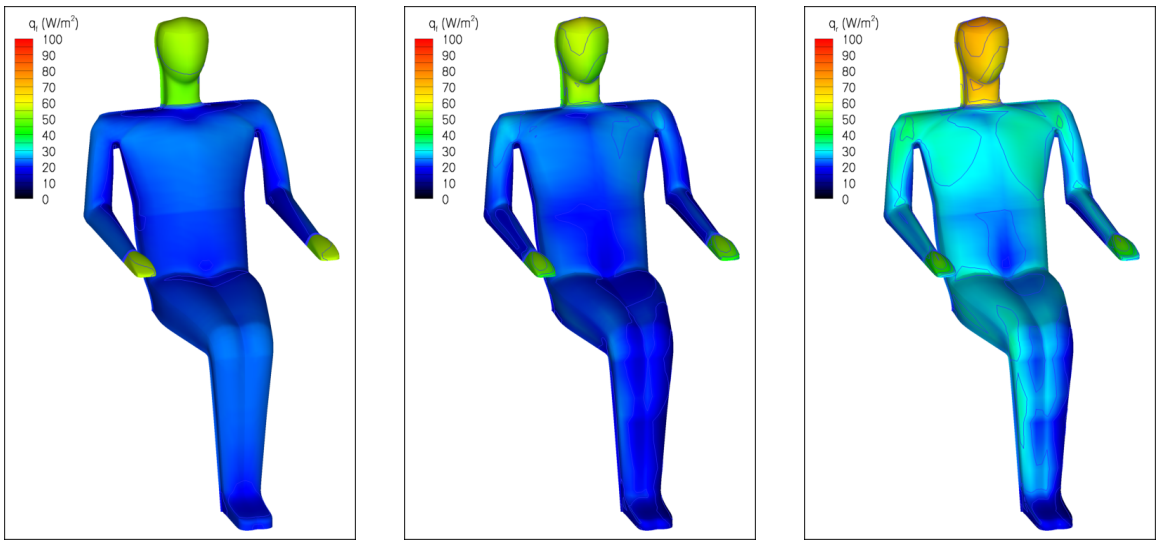

(a) Flow and radiation models with fixed body-surface temperature (of thermoregulation model with ambient temperature $T_{\text{amb}} = 23\ ^\circ\text{C}$)

(b) Coupled system with inflow temperature $T_{\text{ref}} = 23\ ^\circ\text{C}$

(c) Coupled system with inflow temperature $T_{\text{ref}} = 18\ ^\circ\text{C}$

Figure 5: Distribution of net radiation flux for a seated man in a ventilated room.

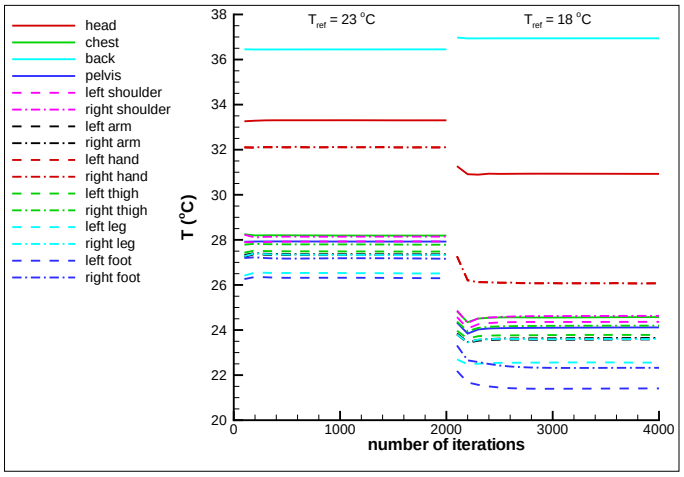

(a) Thermoregulation model

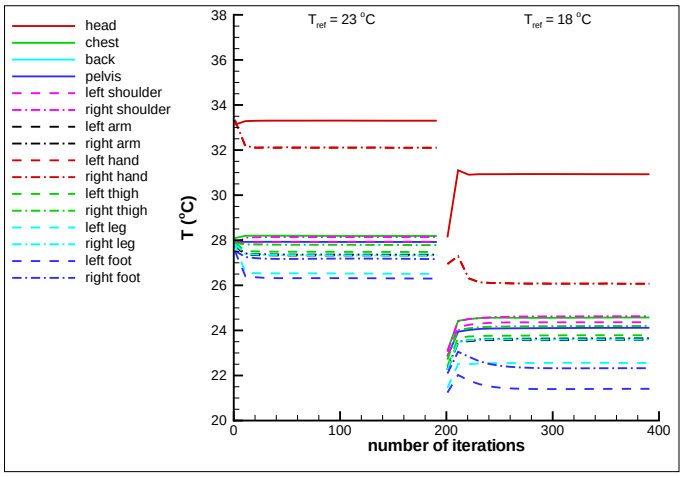

(b) Flow model

Figure 6: Convergence of body-surface temperature for a seated man in a ventilated room.

cabin height	L	$= 2.3\,\mathrm{m}$
gravitational constant	g	$= 9.81\,{}^{\mathrm{m}}/_{\mathrm{s}^2}$
inflow velocity	u_{ref}	$= 0.545\,{}^{\mathrm{m}}/_{\mathrm{s}}$
inflow temperature	T_{ref}	$= 293.15\,\mathrm{K}\ (= 20\,^{\circ}\mathrm{C})$
inflow density	ρ_{ref}	$= 1.205\,{}^{\mathrm{kg}}/_{\mathrm{m}^3}$
specific heat at constant pressure	c_p	$= 1007\,{}^{\mathrm{J}}/_{(\mathrm{kg\,K})}$
dynamic viscosity	μ_{ref}	$= 1.82 \cdot 10^{-5}\,\mathrm{Pa\,s}$
thermal conductivity	λ_{ref}	$= 0.0257\,{}^{\mathrm{W}}/_{(\mathrm{mK})}$
Stefan–Boltzmann constant	σ	$= 5.6704 \cdot 10^{-8}\,{}^{\mathrm{W}}/_{(\mathrm{m^2K^4})}$
emissivity	ε	$= 0.9$

Table 2: Parameters of flow and radiation for cabin with seated passenger.

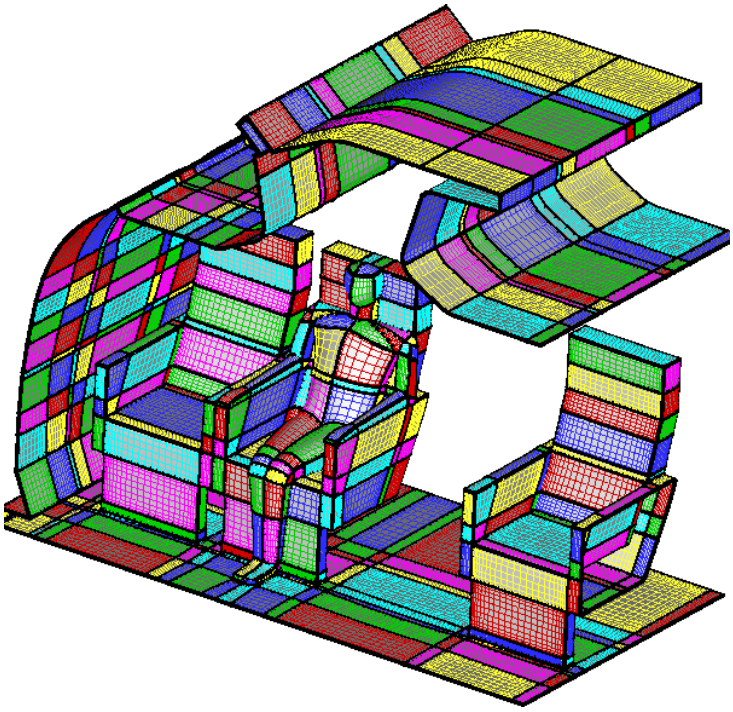

Figure 7: Multi-block structured grid for a cabin with a seated passenger.

Computations are performed on a multi-block structured that consists of 190 blocks and 3.14 million grid cells, illustrated in figure 7. As before, the radiation equations are solved on the surface grid that is one level coarser. The same procedure is followed as for the ventilated room. First, a solution to the original thermoregulation model is determined (with ambient temperature $T_{\text{amb}} = 20\,^{\circ}\text{C}$). Then, the resulting body-surface temperatures are used to solve the flow and radiation models (with an inflow temperature $T_{\text{ref}} = 20\,^{\circ}\text{C}$), and finally a fully coupled simulation is performed.

An impression of the flow solution is given in figure 8. In this case, the air conditioning system blows the air almost directly onto the passenger (most likely, an uncomfortable situation). As a result, the top of the passenger's head appears to be cold. Also his right arm appears to be cooled down by the forced convection.

The body-surface temperature distributions obtained from the original thermoregulation model and from the coupled simulation are shown in figure 9. In this case, contrary to the ventilated room, the coupled simulation results in a lower body temperature than obtained by the original thermoregulation model. This is most likely caused by the air conditioning system blowing directly onto the passenger. The cooling down of the top of the head and the right arm can be seen from the thermal-diffusion heat flux given in figure 10. Finally, the radiation heat flux, which essentially follows the body temperature, is given in figure 11.

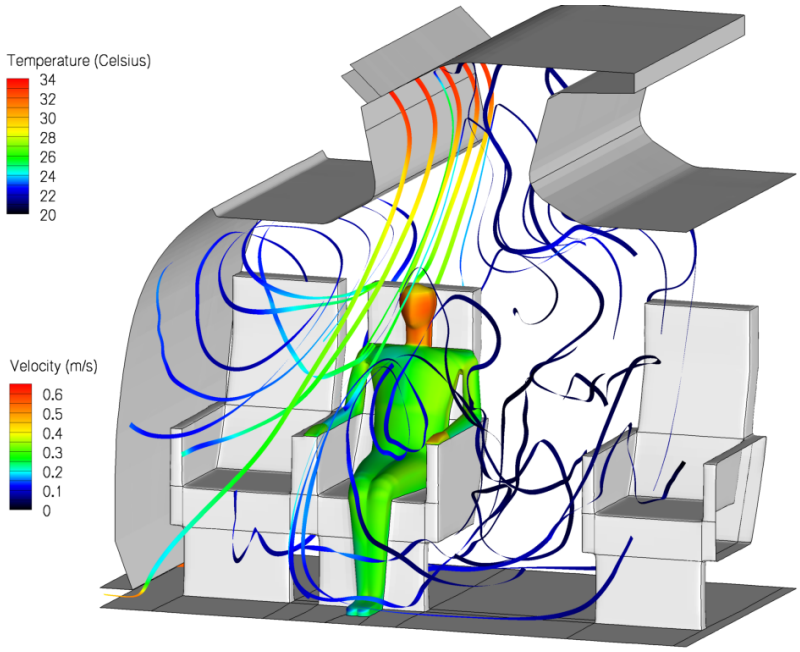

Figure 8: Impression of flow solution for a cabin with a seated passenger. Body surface is coloured with temperature. Stream traces are coloured with local air velocity.

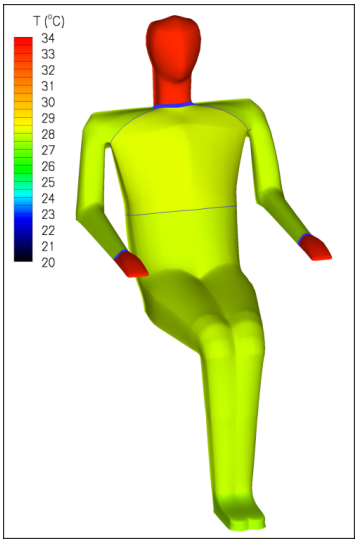

(a) Thermoregulation model with ambient temperature $T_{\text{amb}} = 20\ ^{\circ}\text{C}$

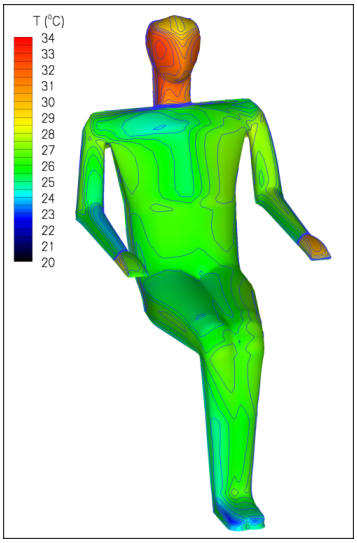

(b) Coupled system with inflow temperature $T_{\text{ref}} = 20\ ^{\circ}\text{C}$

Figure 9: Body-surface temperature distribution of a seated man in an aircraft cabin.

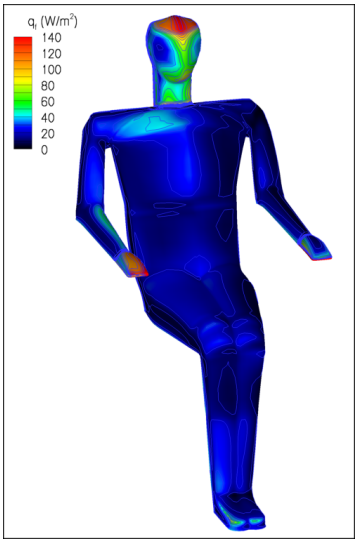

(a) Flow and radiation models with fixed body-surface temperature (of thermoregulation model with ambient temperature $T_{\text{amb}} = 20\ ^\circ\text{C}$)

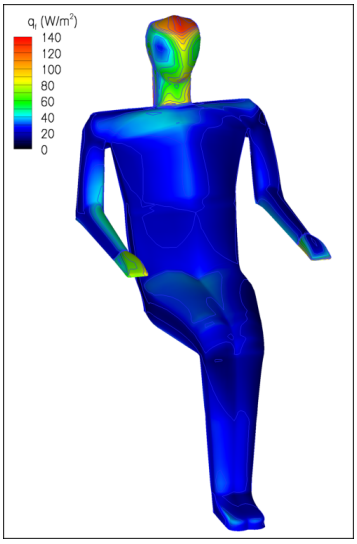

(b) Coupled system with inflow temperature $T_{\text{ref}} = 20\ ^\circ\text{C}$

Figure 10: Distribution of thermal-diffusion heat flux for a seated man in an aircraft cabin.

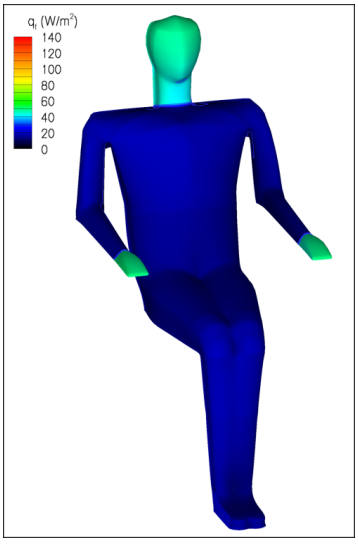

(a) Flow and radiation models with fixed body-surface temperature (of thermoregulation model with ambient temperature $T_{\text{amb}} = 20\ ^\circ\text{C}$)

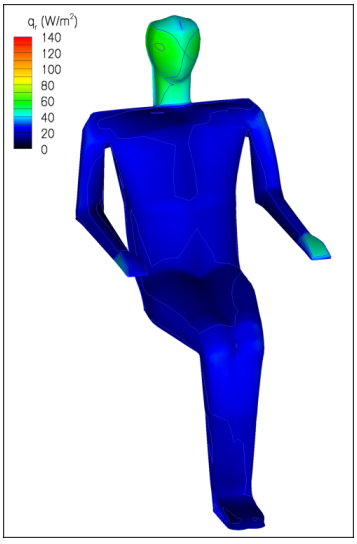

(b) Coupled system with inflow temperature $T_{\text{ref}} = 20\ ^\circ\text{C}$

Figure 11: Distribution of net radiation flux for a seated man in an aircraft cabin.

8 CONCLUSIONS

The development of a simulation environment for studying aspects of individual seat climate has been described. The simulation environment consists of three main elements, viz. a generally applicable state-of-the-art flow model, an existing thermoregulation model to account for human thermal interaction with the environment, and a simplified radiation model suitable for cabin interiors. The three models have been coupled in a robust manner, applying linearizations of the heat flux in order to allow for reliable and efficient solution of the coupled system. The simulation environment has been tested and applied to several academic test cases, for verification and validation purposes, and to more real-life test cases, as presented in this paper, in order to asses the applicability of the simulation environment.

The robustness and efficiency of the coupled methods in the simulation environment is obtained by adding a linearization of the heat flux of the flow field in the boundary conditions of the thermoregulation model, and similarly by adding a linearization of the heat flux of the thermoregulation model in the boundary conditions of the flow model (quasi-simultaneous coupling). Convergence of the resulting, coupled simulation method is shown to be adequate and quick, with the flow solver hardly experiencing convergence delays from the exchange of data with the thermoregulation and radiation models.

The test cases have been used to assess the behaviour of the simulation tool. The tests served to obtain insight into the performance of the simulation environment, in the mutual influence of the models and in the physical basis and properties of the thermoregulation model and the radiation model. Open issues for further research in the models for thermoregulation and internal cabin radiation consist of

- Generalization and flexibility of thermoregulation model (e.g., average person redefinition, individualisation, flexibility in number of segments, impact of cabin pressure)
- Translation to comfort indices
- More advanced radiation model
- Computational effort of third-body shadowing in radiation

In view of the prediction of thermal comfort, it is concluded that the final state of the thermoregulation model from the coupled models in the simulation environment provides a good basis for the determination of thermal comfort.

9 ACKNOWLEDGEMENTS

The work presented in this paper is partially based on work performed within the framework of the European project FACE. The support from the Commission of the European Union, and the cooperation with the partners in the FACE-project are gratefully acknowledged.

REFERENCES

[1] F. Aboosaidi, M.J. Warfield, and D. Choudhury. Numerical analysis of airflow in aircraft cabins. Technical paper 911441, SAE, 1991.

[2] American Society of Heating, Refrigerating, and Air-Conditioning Engineers. *Thermal environmental conditions for human occupancy*, 1992. ANSI/ASHRAE 55-1992.

[3] A.J. Baker, M.B. Taylor, N.S. Winowich, and M.R. Heller. Prediction of the distribution of indoor air quality and comfort in aircraft cabins using computational fluid dynamics (CFD). In N.L. Nagda, editor, *Air quality and comfort in airline cabins*. American Society for Testing and Materials ASTM, 2000.

[4] P.O. Fanger. *Thermal comfort — Analysis and applications in environmental engineering*. McGraw-Hill, 1972. (PhD thesis, TU Denmark, 1970).

[5] D. Fiala, K.J. Lomas, and M. Stohrer. A computer model of human thermoregulation for a wide range of environmental conditions: the passive system. *Journal of Applied Physiology*, (87):1957–1972, November 1999.

[6] D. Fiala, K.J. Lomas, and M. Stohrer. Computer prediction of human thermoregulatory and temperature responses to a wide range of environmental conditions. *International Journal of Biometeorology*, (45):143–159, 2001.

[7] International Organisation for Standardisation. *Moderate thermal environments. Determination of the PMV and PPD indices and specification of the conditions for thermal comfort*, 1995. ISO7730.

[8] J.C. Kok. Resolving the dependence on freestream values for the k–ω turbulence model. *AIAA Journal*, 38(7):1292–1295, 2000. (NLR-TP-99295).

[9] J.C. Kok and S.P. Spekreijse. Efficient and accurate implementation of the k–ω turbulence model in the NLR multi-block Navier–Stokes system. In *Proceedings ECCOMAS 2000*, Barcelona, Spain, 2000. (NLR-TP-2000-144).

[10] R. Siegel and J.R. Howell. *Thermal radiation heat transfer*. Taylor & Francis, 4th edition, 2002. (The enclosed configuration factor catalog is also available at http://www.me.utexas.edu/ howell).

[11] J.A.J. Stolwijk. Mathematical model of thermoregulation. In Hardy, Gagge, and Stolwijk, editors, *Physiological and Behavioral Temperature Regulation*, chapter 48, pages 703–721. Charles C. Thomas Publication, 1970.

[12] J.A.J. Stolwijk. A mathematical model of physiological temperature regulation in man. NASA Contractor Report CR-1855, NASA, 1971.

[13] S. Tanabe, K. Kobayashi, J. Nakano, Y. Ozeki, and M. Konishi. Evaluation of thermal comfort using combined multi-node thermoregulation (65MN) and radiation models and computational fluid dynamics (CFD). *Energy and Buildings*, 34:637–646, 2002.

[14] E. Turkel. Preconditioned methods for solving the incompressible and low speed compressible equations. *Journal of Computational Physics*, 72:277–298, 1987.

[15] E. Turkel. Preconditioning techniques in computational fluid dynamics. *Annual Review of Fluid Mechanics*, 31:385–416, 1999.

[16] E.H. Wissler. Mathematical simulation of human thermal behavior using whole body models. In *Heat transfer in medicine and biology, analysis and applications*. Plenum Press, New York, 1985.